ADVANCED FUNCTIONAL MATERIALS
www.afm-journal.de

Resonant-Enhanced Full-Color Emission of Quantum-Dot-Based Display Technology Using a Pulsed Spray Method

Kuo-Ju Chen, Hsin-Chu Chen, Kai-An Tsai, Chien-Chung Lin, Hsin-Han Tsai, Shih-Hsuan Chien, Bo-Siao Cheng, Yung-Jung Hsu, Min-Hsiung Shih, Chih-Hao Tsai, His-Hsin Shih, and Hao-Chung Kuo**

Colloidal quantum-dot light-emitting diodes (QDLEDs) with the HfO_2/SiO_2-distributed Bragg reflector (DBR) structure are fabricated using a pulsed spray coating method. Pixelated RGB arrays, 2-in. wafer-scale white light emission, and an integrated small footprint white light device are demonstrated. The experimental results show that the intensity of red, green, and blue (RGB) emission exhibited considerable enhancement because of the high reflectivity in the UV region by the DBR structure, which subsequently increases the use in the UV optical pumping of RGB QDs. A pulsed spray coating method is crucial in providing uniform RGB layers, and the polydimethylsiloxane (PDMS) film is used as the interface layer between each RGB color to avoid cross-contamination and self-assembly of QDs. Furthermore, the chromaticity coordinates of QDLEDs with the DBR structure remain constant under various pumping powers in the large area sample, whereas a larger shift toward high color temperatures is observed in the integrated device. The resulting color gamut of the proposed QDLEDs covers an area 1.2 times larger than that of the NTSC standard, which is favorable for the next generation of high-quality display technology.

1. Introduction

Recently, colloidal quantum-dot light-emitting diodes (QDLEDs) have been rapidly developed for display applications because of their narrow bandwidths, high luminescence efficiency, broad absorption, and size-engineered band gap. They are particularly promising as light sources of illumination in display applications to replace traditional cold-cathode fluorescent lamps (CCFL).[1–4] The common approach to fabricate white LEDs is to combine the InGaN blue chip with phosphor, which exhibits high quality performance in the visible light and fixed emission spectra.[5] As a novel technology in this field, QDs offer more varieties in color mixing. In the past, high quantum efficiency and an excellent color-rendering index were achieved by multishell QDs and co-doping QDs in phosphor.[6,7] Moreover, the first use of QD light emission in a display was demonstrated by crosslinking the colloidal quantum-dot layer.[8] Although promising results were obtained, issues such as cross-contamination between colors and the inefficient utilization of raw QD materials occur among various deposition technologies, such as spin coating, mist coating, and inkjet printing.[9–12] Because of the design of the deposition chamber in the mist coating method, the actual deposited volume of active material (such as quantum dots) is less than 10% of the overall disposal, which leads to a waste of material.[12] Another inevitable disadvantage is the so-called coffee ring effect, which is caused by migration of the solutes toward the edge of the droplets during drying.[13] The inkjet printing method has been demonstrated as a feasible method of QD device fabrication in the deposition of the substrate because of its simplicity and low cost; however, it produces non-uniform surfaces and inaccurate patterning.[14] The separation of each RGB pattern and the uniformity of RGB colors are critical conditions to obtain successful QDLEDs in industrial applications.

The optimal solution to these problems is the pulsed spray coating method, which can be used with an interval control through an air atomizing nozzle to control the thickness of the QD layer by layer.[15] The cross-contamination in red-green-blue (RGB) pixels can be alleviated using polydimethylsiloxane

K.-J. Chen, H.-C. Chen, H. H. Tsai, S.-H. Chien, B.-S. Cheng, Prof. H.-C. Kuo
Department of Photonic & Institute of Electro-Optical Engineering
National Chiao Tung University
Hsinchu 30010, Taiwan
E-mail: hckuo@faculty.nctu.edu.tw
K.-A. Tsai, Prof. Y.-J. Hsu
Department of Materials Science and Engineering
National Chiao Tung University
1001 University Road, Hsinchu 30010, Taiwan
Prof. C.-C. Lin
Institute of Photonic System
College of Photonics
National Chiao Tung University
No.301, Gaofa 3rd Rd., Guiren Dist., Tainan City 71150, Taiwan
E-mail: chienchunglin@faculty.nctu.edu.tw
Prof. M.-H. Shih
Research Center for Applied Sciences
Academia Sinica 128 Academia Rd., Sec. 2 Nankang, Taipei 115, Taiwan
Dr. C.-H. Tsai, Dr. H.-H. Shih
Chi Lin Optoelectronics Co., Ltd, Tainan, Taiwan

DOI: 10.1002/adfm.201200765

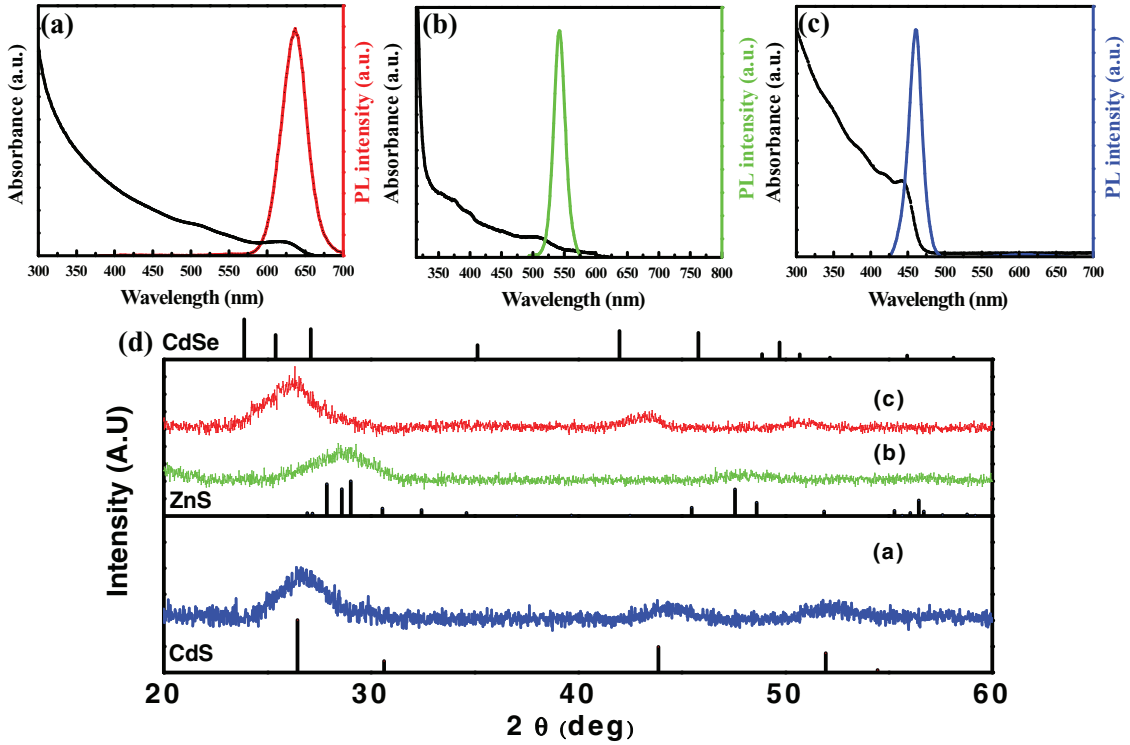

Figure 1. UV-visible absorption and PL emission spectra of QDs with the emission colors of a) red, b) green, and c) blue. The corresponding XRD patterns are shown in (d). In (d), the reference patterns of wurtzite CdSe (JCPDS 77-0021), wurtzite ZnS (JCPDS 72-0163), and cubic CdS (JCPDS 65-2887) are also included for comparison.

(PDMS) as the interface layer to separate each RGB color. PDMS has a high degree of transparency, stability, and flexibility, which is suitable for the substrate of RGB pixelated arrays and full color in QDLEDs.

This study fabricated large-area and small footprint QDLEDs by dispensing the QD layer by using the pulsed spray coating method. Furthermore, HfO_2/SiO_2 DBR with a stopband centered at 400 nm and a full width of approximately 60 nm was used to enhance the use of UV pumping photons, thereby increasing RGB emission intensity. Consequently, this combination of RGB QDs with highly reflective DBR exhibits high color purity and provides an alternative method for display applications.

2. Analysis of QDs

The optical properties of three QD products purchased from Sigma-Aldrich were first characterized using UV-visible absorption and photoluminescence (PL) spectroscopy. As shown in **Figure 1**, both red and blue QDs exhibited an absorption edge that is consistent with the bulk band gap energy of CdSe (E_g = 1.7 eV) and CdS (E_g = 2.5 eV). This result was consistent with that of X-ray diffraction (XRD) analysis, in which the observed diffraction peaks were identified as wurtzite CdSe and cubic CdS. For QDs that emit green, an absorption onset located between the band gap energy of ZnS (E_g = 3.7 eV) and CdSe was observed, indicating the existence of an alloyed structure of $Cd_{1-x}Zn_xSe_{1-y}S_y$. The corresponding XRD pattern showed the diffraction behavior of wurtzite ZnS, with an apparent shift of the main peak caused by alloying with CdSe. The low intensity and low signal-to-noise ratio of XRD data were mainly attributed to the small size and inferior crystallinity of QDs.[16,17] The small number of QDs applied in XRD measurement also contributed to this low spectral intensity. The PL spectra of the three samples exhibited band-to-band emission bands centered at 635, 540, and 460 nm for CdSe, $Cd_{1-x}Zn_xSe_{1-y}S_y$, and CdS QDs, respectively.

Further structural characterizations were performed using a transmission electron microscope (TEM) and high-resolution TEM (HRTEM). **Figure 2**a,c,e show the typical TEM images with the corresponding selected-area electron diffraction (SAED) patterns of the three QD samples. These QD samples were considerably uniform in morphology and exhibited a narrow size distribution. The average diameter of red, green, and blue QD samples was measured as 5.41 ± 0.34 nm, 4.16 ± 0.21 nm, and 3.58 ± 0.22 nm, respectively. The line width of PL for red, green, and blue QDs was 38.4, 20.3, and 20.5 nm, respectively. Because red QDs have a relatively wide size distribution of 6.3%, they exhibited a broader PL line-shape than blue and green QDs. The inset SAED patterns confirm the crystal structure deduced from XRD analysis. Figure 2b,d,f show the detailed crystallographic structures of the three QD samples. These lattice-resolved images reveal the lattice planes.

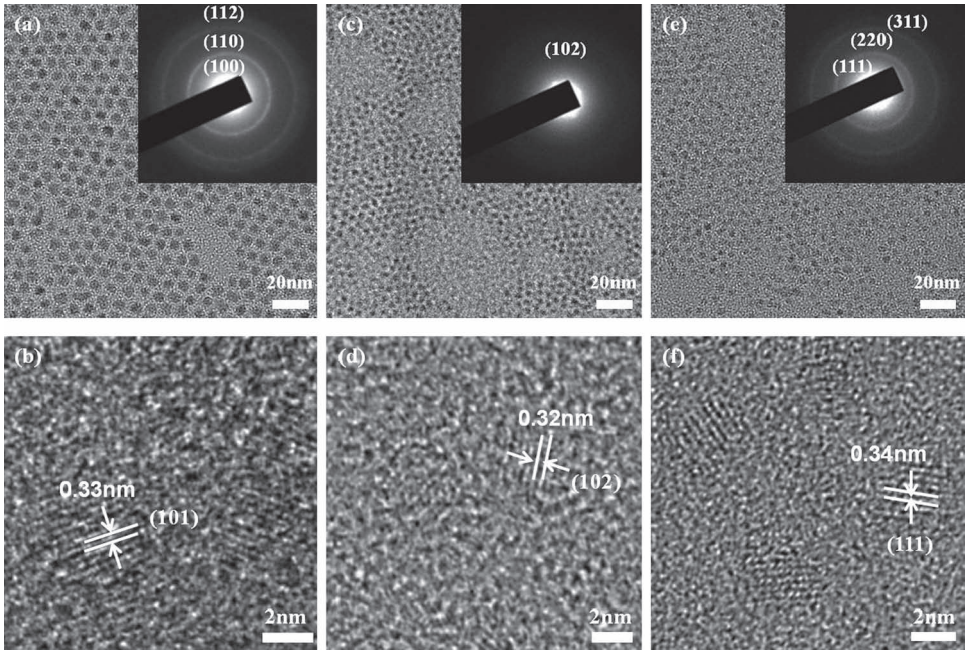

Figure 2. Typical TEM images of QDs with the emission colors of a) red, c) green, and e) blue. The corresponding HRTEM images are shown in (b), (d), and (f), respectively.

3. Large Area Sample Results

A simple large area sample was first fabricated to verify our idea. Multiple layers of PDMS film were made separately, and deposition of CQDs was performed between PDMS stacking layers. As described in the Experimental section, an 11-pair HfO_2/SiO_2 DBR thin-film structure was placed on top of the sample. In the DBR structure, the maximal reflectivity was designed for a UV wavelength of approximately 400 nm, and the refractive index of the HfO_2 and SiO_2 layers were 1.9 and 1.46, respectively. Over 90% of reflectivity can be maintained between 365 nm and 430 nm; the wavelength of the UV source was 380 nm. By contrast, the reflectivity was lower in the visible spectral range. The mirror stack was designed to enable SiO_2/HfO_2 DBR to reflect most of the UV light and transmit the visible photons. Therefore, the reflected UV photons excited more RGB QDs and increased the efficiency of pumping.

Figure 3a shows the relative intensity of the large-area samples with DBR under a driving current of 350 mA in a UV pumping LED, compared with the reference without DBR. The result demonstrates that the large-area samples with DBR have higher intensity in red, blue, and green components than the reference without DBR. The reflection of light from the DBR structure can enhance the efficiency because the increased light path leads to a higher possibility of exciting the RGB QDs. The CIE color coordinates of the large-area samples with DBR, which provide a white light output, are (0.29, 0.29) shown in the inset of Figure 3a. To further verify the pumping power dependence of each color, the driving current of the UV LED was varied from 100 mA to 400 mA. The enhancement of each color from the DBR sample over the non-DBR sample is shown in Figure 3b. A saturation of this enhancement ratio was observed among red, green, and blue QD emissions beyond 250 mA, which indicates a possible quench in the quantum yield of the quantum dots. Additionally, the enhancement ratio of red emission was higher than that of the other colors, which can be attributed to the proximity of red QD layers to the UV source. Although the transparency in PDMS is high, slight UV light loss occurs in each PDMS layer. However, PDMS performs a crucial role in separating the RGB QDs in our structure, and can further isolate the air from RGB QDs, which can stop the

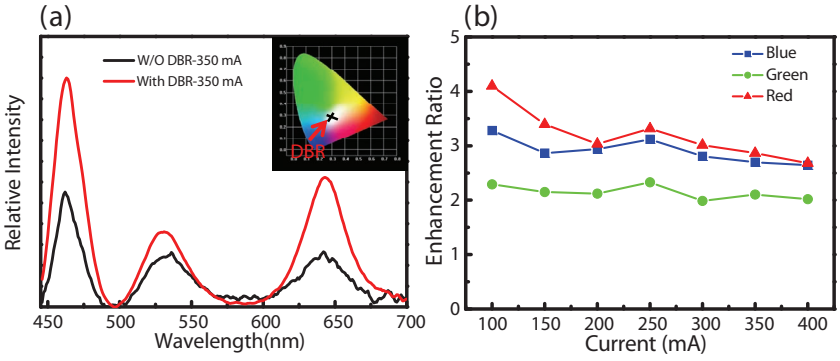

Figure 3. a) The relative intensity of the large-area samples with and without DBR operated under 350 mA. The inset shows the CIE color coordinates of the large-area samples with DBR. b) Enhancement ratio of the intensity of large-area samples with and without DBR under various currents from 100 to 400 mA.

Table 1. The relative illumination intensity and absorption of the RGB QDs after spraying on the surface of the glass.

	Red	Green	Blue
Relative intensity [%]	100	11	60
Absorption at 380 nm [%]	8.8	2.3	4.7

intensity degradation in RGB QDs. The green QDs exhibited a weaker enhancement in general. This may have been caused by the substantial aggregation of green QDs when they were sprayed and dried on the substrate. When dispersed and dried on a glass substrate, green QDs exhibited pronounced PL depression, whereas red and blue QDs retained comparable PL intensities, as shown in **Table 1**. This phenomenon indicates that green QDs experienced considerable aggregation during the solidification process, which is the main cause for the lower enhancement ratio observed for the LED. Further information can be acquired from the absorption spectrum. A smaller absorption of the green dot was observed from the direct measurement of reflection and transmission on solidified quantum dots on glass (Table 1), which also indicates a possible decrease in UV excitation efficiency.

The chromaticity coordinate of the large-area samples with DBR remained almost the same with the increase of the driving current, which indicates that the large-area sample with the DBR structure has high stability in color rendering, and this characteristic is crucial in solid-state lighting. With this pump-power-independent color mixing, our PDMS-layered structure can provide a tunable color-rendering scheme by adjusting the quantities of the RGB QDs of each layer. Additionally, the CIE coordinates of the large-area samples with DBR were compared to the National Television System Committee (NTSC) standard color triangle. The RGB color coordinates for the large-area samples with DBR were (0.69, 0.3), (0.19, 0.75), and (0.13, 0.05). Therefore, the area of the RGB triangle of the large-area samples with DBR was enhanced by 20%, compared to the NTSC color gamut. This result can be attributed mainly to the narrow bandwidth in the RGB QDs, which have high color purities.

The images of the pixelated structure and 2-in. full-wafer sample under UV excitation are shown in **Figure 4**. The size of each pixel was 2 mm × 2 mm, as shown in Figure 4a, which can be scaled up and down according to the application.

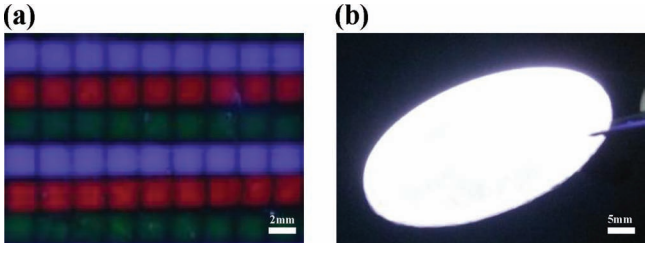

Figure 4. Image of the a) pixel pattern and b) a 2-in. full wafer structure under UV excitation.

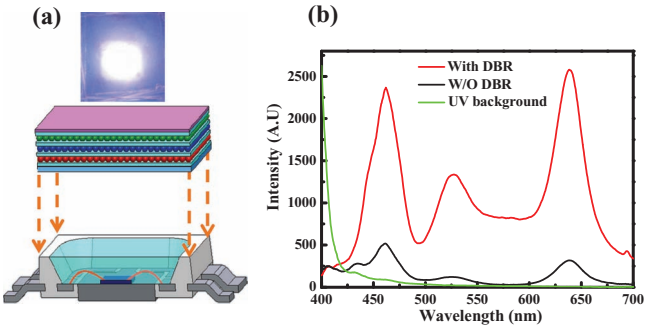

Figure 5. a) Top: the QDLED device in action; bottom: the device schematic diagram. b) EL spectra with and without the DBR structure.

Figure 4b shows the full-size white light source under UV excitation.

4. Integrated Device Results

After finishing the large area test, we further shrank the scale to an actual LED package. **Figure 5**a shows the schematic diagram of QDLED and a picture of a real QDLED in operation. Figure 5b shows the electroluminescence (EL) spectra of our QDLED with and without the DBR structure. The background of pure UV LED emission is also shown in the figure. Three emission peaks occurred at 460 nm (blue band), 530 nm (green band), and 640 nm (red band), which were contributed by the RGB QDs. This indicated that EL with the DBR has stronger visible emission than that without the DBR structure.

The normalized EL spectra of UV chips with the DBR structure from 50 mA to 350 mA are shown in **Figure 6**a. Higher RGB emission can be obtained by increasing the current, thereby achieving higher intensity. The chromaticity coordinates at various drive currents are shown in the inset of Figure 6a, and are marked by a red trace on the CIE map. Compared to our large-area installation, which exhibited almost no change in CCT, the integrated LED device demonstrated higher current dependence, which may have been caused by the thermal conduction problem inside the package. The luminous efficacy of radiation (LER) was calculated using the following formula:[18,19]

$$\mathrm{LER} = 683\frac{lm}{W}\frac{\int_{\lambda} P_{\mathrm{white}}(\lambda)\,V(\lambda)\mathrm{d}\lambda}{\int_{\lambda} P_{\mathrm{white}}(\lambda)\mathrm{d}\lambda} \quad (1)$$

where 683 lm/W is a normalization factor, $P_{\mathrm{white}}(\lambda)$ is the spectral power density of the light source, and $V(\lambda)$ is the human eye sensitivity function. The final results of the DBR sample and no-DBR sample are shown in Figure 6b, which shows the superior performance of the DBR sample over all currents. Conversely, if the absolute intensity of emission is graphed against the driving current, the relative intensity rolls over beyond 350 mA because of the UV LED power saturation and the drop in quantum-dot efficiency with increasing temperature inside the package.

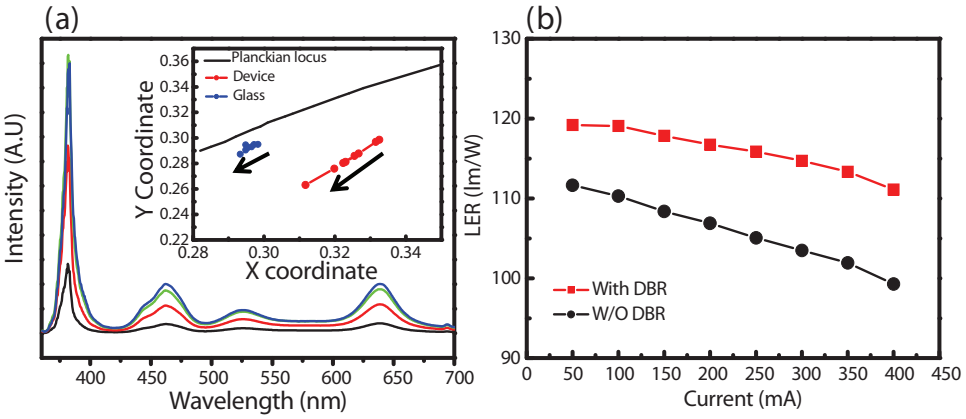

Figure 6. a) The relative emission spectrum of the QDLED with a DBR structure under various drive currents (50, 150, 250, and 350 mA, from bottom to top curves). The inset is the zoomed-in CIE1931 chromaticity diagram with traces of our QD material when dispensed on glass or packaged in the QDLED format under various pumping powers (for glass) or drive currents (for the QDLED device). b) The luminous efficacy of optical radiation of UV chips with a DBR structure under currents between 50 mA and 400 mA.

5. Conclusion

In conclusion, this study demonstrated an integrated platform of colloidal quantum dots, UV LEDs, PDMS multiple layers, and DBR stacks that can achieve enhanced performance of full-color white light emission. Both large area and micrometer scale integrated devices were demonstrated. With the addition of UV DBR stacks, the use of pumping UV photons can be enhanced, which increases the output power of RGB. Furthermore, the chromaticity coordinates of the large-area samples with DBRs remained pump-power-independent, whereas those of the integrated device exhibited a larger shift under elevated pumping power because of possible thermal issues. Finally, QDLEDs with the DBR structure fabricated using the pulsed spray coating method demonstrated an excellent optical characteristic with high stability, which can provide an alternative approach in display technology.

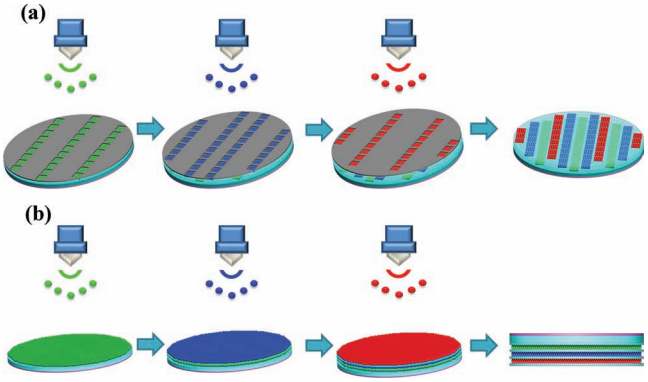

Figure 7. Schematic illustration of a) pixelated arrays and b) full-color by pulsed spray coating method.

6. Experimental Section

Pulse Spray Method: The pulsed spray (PS) coating method was used to spray the RGB QD layers.[20] In traditional spraying techniques, the viscosity of the spraying mixtures can considerably affect the uniformity of the finished film. The interaction between the particles in the premixed solution can cause a gathering of the materials, and self-clustering can block the passage of the spray. The PS method can improve this issue using two special designs, that is, using the air-injection mechanism in the nozzle and intermittent spraying frequency (5 to 10 Hz), and using the constant stirring system. These methods can separate the target particles in the suspending solution more effectively than traditional methods. Thus, the atomized mixture of quantum dots and solvent can pass through a tiny nozzle to reach the desired surface, further reducing the chances of quantum-dot self-assembly. The actual operation was precisely controlled by a computer network, and the quantity of the spray can be monitored.

Large-Area Device Fabrication: **Figure 7** shows the process flowcharts of the pixelated RGB QD arrays and non-patterned white light source on a 2-in. substrate. The concentrations of the RGB QD were approximately 1 mg/ml. The pixelated arrays shown in Figure 7 were fabricated using the following steps: 1) an 11-pair HfO_2/SiO_2 DBR was evaporated in an ion-assisted e-gun system on the top of the glass; 2) the mask was placed on the top of the substrate for alignment; and 3) the RGB QDs were sprayed onto the surface of the glass in the sequence of green, blue, and red. Similar steps can be followed for a 2-in. wafer white light source; however, no mask alignment is used.

The PDMS pre-polymer solution was poured over the glass substrate using the spin-coating method at 700 rpm for 60 s, and baked in an oven at 70 °C. Subsequently, the PDMS film was ready for peeling. The thickness of the PDMS layer measured using SEM was approximately 80 μm. Because each PDMS layer was processed using the same parameters, we ensured that each layer in our structure had the same thickness. The thickness of the QD layer was difficult to measure because of the considerable thickness difference between the PDMS and the QD layer; only the TEM technique was used when they were manually dropped and dried. From the TEM image, we estimated the QD layer thickness at approximately 50 to 70 nm.

Depending on the application, wafer-scale white color and RGB pixelated arrays can be easily deposited on the substrate with or without a mask. The mask in our experiment was composed of an aluminum plate, and we opened an array of square (2 mm × 2 mm) holes. The interval of the each pixel was 5.22 mm. The alignment between the various colors can be achieved by visual inspection and XY translational stage adjustment. In the pulsed spray procedure, the air pressure of the gun was approximately 0.5 MPa, and the pressures of the atomized air and swirl air were approximately 0.2 MPa.

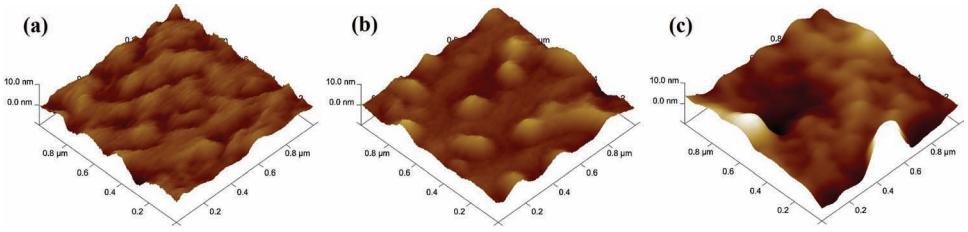

Figure 8. AFM image of the a) blue, b) green, and c) red QD layer by pulsed spray coating method.

After PS QD deposition, we measured the AFM images of the surface, as shown in **Figure 8**. The QDs aggregated and clustered after layer-by-layer deposition. The AFM measurement of the blue, green, and red QD layer revealed a root-mean-square (RMS) roughness of 1.18, 0.816, and 0.788 nm, respectively. The RMS results indicate that uniform dispensing is possible with this technology.

Integrated Device Fabrication: The integrated white light QDLED has similar process steps to create QD+PDMS+DBR structures. A large-area multiple-layer structure was cut into smaller pieces to fit the lead frame of the UVLED SMD5070 package. The size of the UV-LED lead frame was 5 mm × 5 mm, and the size of the square chips was 45 mil by 45 mil. The chip was made of InGaN multiple quantum wells with AlGaN barriers. The UV-LED chips with an emission wavelength of 380 nm were bonded on silver glue with gold wire, and its radiant fluxes were approximately 54 mW at 300 mA. The voltage of the UV-LED chips was approximately 3.96 V. The direct attachment of the QD layers to the UVLED frame yielded a smaller device form factor that can be applicable in the real world.

Characterizations: The morphology and dimensions of the quantum dots purchased from Sigma-Aldrich were examined using a TEM (JEOL, JEM-2100) operated at 200 kV. The crystallographic structures of the samples were investigated using XRD (MAC Science, MXP18) and HRTEM (JEOL, JEM-3000) operated at 300 kV. The UV-visible absorption spectra were obtained using a Hitachi U-3900H spectrophotometer at room temperature. A Hitachi F-4500 equipped with a xenon lamp (150 W) was used for PL spectroscopy.

Acknowledgements

The authors would like to thank Chi Lin Optoelectronics for their technical support and Prof. S. C. Wang, Prof. T. C. Lu, and Prof. P. Yu for their suggestions. Y.J.H. appreciates the financial support from National Science Council of Taiwan under grant NSC-100-2113-M-009-004. C.C.L. would like to acknowledge the financial support of National Science Council of Taiwan through contract number NSC99-2221-E-009-052-MY3. H.C.K. and C.C.L. would also like to thank the Advanced Optoelectronic Technology Center, National Cheng Kung University for support.

Received: March 19, 2012
Revised: June 18, 2012
Published online: August 1, 2012

[1] Q. Sun, Y. A. Wang, L. S. Li, D. Wang, T. Zhu, J. Xu, C. Yang, Y. Li, *Nat. Photonics* **2007**, *1*, 717.
[2] S. Coe, W. K. Woo, M. Bawendi, V. Bulovic, *Nature* **2002**, *420*, 800.
[3] Y. J. Lee, C. J. Lee, C. M. Cheng, *Opt. Express* **2010**, *18*, A554.
[4] H. Song, S. Lee, *Nanotechnology* **2007**, *18*, 255202.
[5] S. Nizamoglu, T. Ozel, E. Sari, H. V. Demir, *Nanotechnology* **2007**, *18*, 065709.
[6] E. Jang, S. Jun, H. Jang, J. Llim, B. Kim, Y. Kim, *Adv. Mater.* **2010**, *22*, 3076.
[7] H. S. Jang, H. Yang, S. W. Kim, J. Y. Han, S. G. Lee, D. Y. Jeon, *Adv. Mater.* **2008**, *20*, 2696.
[8] K. S. Cho, E. K. Lee, W. J. Joo, E. Jang, T. H. Kim, S. J. Lee, S. J. Kwon, J. Y. Han, B. K. Kim, B. L. Choi, J. M. Kim, *Nat. Photonics* **2009**, *3*, 341.
[9] J. L. Zhao, J. A. Bardecker, A. M. Munro, M. S. Liu, Y. H. Niu, I. K. Ding, J. D. Luo, B. Q. Chen, A. K. Y. Jen, D. S. Ginger, *Nano Lett.* **2006**, *6*, 463.
[10] T. Zhu, K. Shanmugasundaram, S. C. Price, J. Ruzyllo, F. Zhang, J. Xu, S. E. Mohney, Q. Zhang, A. Y. Wang, *Appl. Phys. Lett.* **2008**, *92*, 023111.
[11] V. Wood, M. J. Panzer, J. Chen, M. S. Bradley, J. E. Halpert, M. C. Bawendi, V. Bulovic, *Adv. Mater.* **2009**, *21*, 2151.
[12] H. M. Haverinen, R. A. Myllyla, G. E. Jabbour, *Appl. Phys. Lett.* **2009**, *94*, 073108.
[13] A. Kshirsagar, S. Pickering, J. Xu, J. Ruzyllo, *ECS Trans.* **2011**, *35*, 71.
[14] T. H. Kim, K. S. Cho, E. K. Lee, S. J. Lee, J. Chae, J. W. Kim, D. H. Kim, J. Y. Kwon, G. Amaratunga, S. Y. Lee, B. L. Choi, Y. Kuk, J. M. Kim, K. Kim, *Nat. Photonics* **2011**, *5*, 176.
[15] H. C. Kuo, C. W. Hung, H. C. Chen, K. J. Chen, C. H. Wang, C. W. Sher, C. C. Yeh, C. C. Lin, C. H. Chen, Y. J. Cheng, *Opt. Express* **2011**, *19*, A930.
[16] S. Neeleshwar, C. L. Chen, C. B. Tsai, Y. Y. Chen, C. C. Chen, S. G. Shyu, M. S. Seehra, *Phys. Rev. B* **2005**, *71*, 201307.
[17] P. Thangadurai, S. Balaji, P. T. Manoharan, *Nanotechnology* **2008**, *19*, 435708.
[18] S. Nizamoglu, T. Erdem, X. W. Sun, H. V. Demir, *Opt. Lett.* **2010**, *35*, 3372.
[19] T. Erdem, S. Nizamoglu, X. W. Sun, H. V. Demir, *Opt. Express* **2010**, *18*, 340.
[20] H. T. Huang, C. C. Tsai, Y. P. Huang, *Opt. Express* **2010**, *18*, A201.